

IMPACT MELT AND MAGMATIC PROCESSES IN CENTRAL SOUTH POLE - AITKEN BASIN. D. P. Moriarty III¹ and C. M. Pieters¹, ¹Department of Earth, Environmental, and Planetary Sciences, Brown University, Providence, RI 02912 [Daniel_Moriarty@Brown.edu]

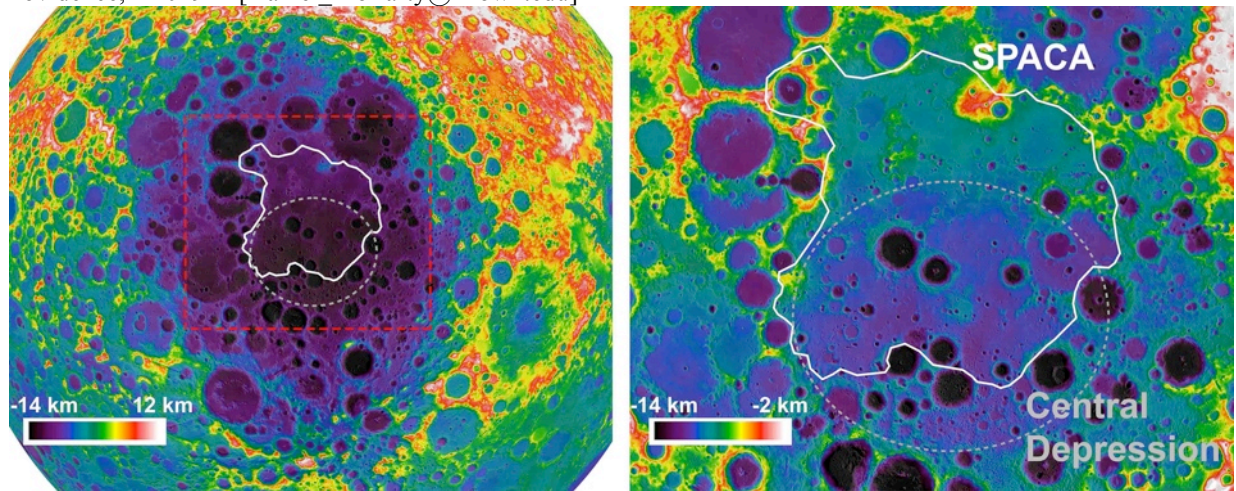


Fig. 1: LOLA[11] topography centered on SPA at two scales. The central depression and SPACA region are outlined.

Introduction: The tremendous energy imparted during formation of the vast South Pole - Aitken Basin (SPA) melted and excavated large volumes of deep-seated materials[1-5]. Compositionally, the SPA interior exhibits elevated Th and Fe[6] and non-mare areas are dominated by Mg-rich pyroxenes (norites)[7,8]. However, the center-most portion of SPA exhibits a composition containing higher-Ca pyroxenes[9]. In this analysis, we investigate the composition and geology of this "Central SPA Compositional Anomaly"(SPACA) using M^3 spectra[10], LOLA topography[11], and LROC imagery[12].

SPACA: Physical properties. The center-most region of SPA is associated with a roughly elliptical area of low topography ~ 560 km across, as seen in Fig. 1. Throughout this central depression, the basin floor is relatively smooth and appears to exhibit a paucity of impact craters. A lower crater density compared to other portions of the SPA interior is confirmed using a LOLA-derived catalog of craters ≥ 20 km[13,14].

This crater-deficient smooth terrain is not confined to the center-most depression; it extends to the north across an irregular region with slightly higher topography. Across this central depression and irregular smooth terrain, several superposed craters ($< \sim 50$ km) appear buried, filled, or otherwise modified[15].

Compositional properties. The mineralogy of SPACA is distinct from elsewhere in the basin. Spectral variations across SPA are dominated by the abundance and composition of pyroxenes. Therefore, compositional diversity across the basin can be evaluated using the $1 \mu\text{m}$ and $2 \mu\text{m}$ absorption band centers [16-18]. A map of the $1 \mu\text{m}$ band centers of mafic materials exhibiting $1 \mu\text{m}$ band depths $> 10\%$ is given in Fig. 2. In general,

noritic materials exhibit the shortest-wavelength band centers (blue), while mare basalts exhibit the longest-wavelength band centers (red) as well as a low albedo. Example spectra of these materials are given in Fig. 3.

Outlined in Fig. 2, SPACA is a region ~ 700 km across in central SPA that does not resemble norites or mare basalts. SPACA materials (excluding small, localized mare deposits) exhibit similar but slightly shorter-wavelength band centers than mare materials but are generally brighter (Fig. 3). These spectral properties imply a clinopyroxene-bearing lithology with an average pyroxene composition slightly lower in Ca,Fe than typical mare basalts.

This distinctive lithology is pervasive in the walls of craters from small (< 1 km) to large (e.g. Bhabha (64 km diameter), Finsen (72 km), Stoney (45 km), and White (39 km)). Based on crater scaling relationships[4], this indicates a compositionally uniform zone at least several km thick. On the other hand, several central peaks in this region (e.g. Finsen, Bhabha, Stoney) expose a noritic composition. Since central peaks represent the deepest material sampled by any given crater[19], this sets an upper limit of ~ 10 km on the thickness of the SPACA deposit.

Possible Origin of the SPACA: Impact melt. Impact models suggest that the SPA-forming impact produced large volumes of impact melt dominated by mantle materials[5]. Although the bulk composition might therefore be dominated by olivine or orthopyroxene[20], differentiation of such melt could produce a near-surface layer of cpx-bearing materials overlying more noritic materials, under certain conditions[21]. Based on equations in[22], a ~ 50 km thick SPA melt sheet[23] would crystallize in ~ 5 myr. Due to volume changes during cooling and crystallization, thick impact melt sheets are expected to vertically shrink by $\sim 10\%$

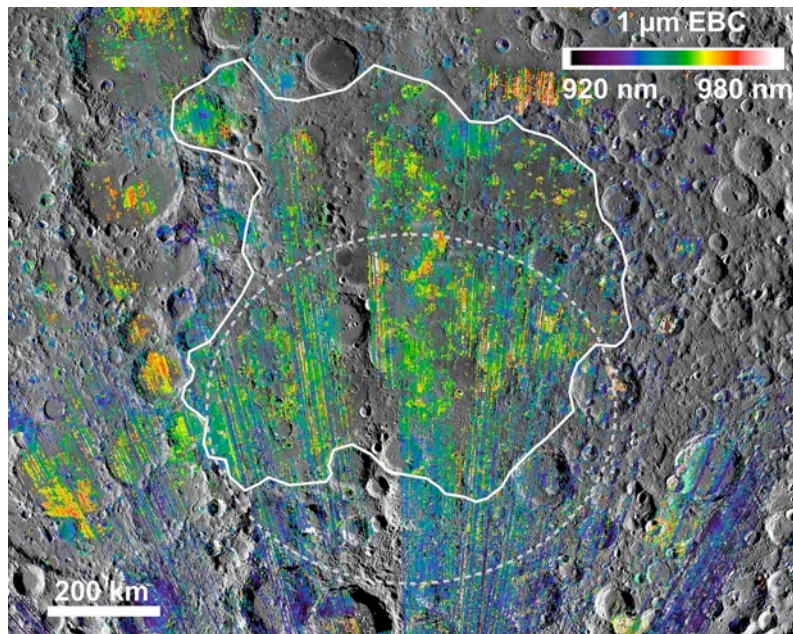


Fig. 2: M^3 -derived $1 \mu\text{m}$ absorption band center (EBC) overlaid on a WAC image mosaic. The approximate extents of the central depression (dashed) and SPACA (solid) are given.

when fully crystallized[22]. In basins such as Orientale, this is thought to produce a roughly elliptical central depression[22]. The ~ 560 km central depression in SPA may be an analogous structure. If so, this outlines the extent of the thickest, most coherent part of the SPA melt sheet - the portion most likely to differentiate.

Volcanic flooding. Localized mare and cryptomare deposits have been identified across SPA[7,24,25]. However, the character of SPACA is more continuous than these localized mare. Additionally, SPACA is compositionally distinct from SPA mare basalts, exhibiting slightly shorter-wavelength absorption bands as well as a higher albedo (Fig. 3). If SPACA is volcanic in origin, it may represent different magmatic processes than those that produced mare basalts.

Geophysical models suggest that large impacts can trigger localized convection and subsequent melting, especially for thin lithospheres and warm mantle temperatures[26]. This melting can occur over tens of myr[26], an order of magnitude (or more) longer than the cooling of the SPA melt sheet. This delayed impact-induced melting might result in lava emplacements similar to terrestrial flood basalts[26]. These flood basalts exhibit compositional signatures that reflect differences in melting conditions[27]. Similarly, melts geophysically triggered by SPA occur under different conditions and may be compositionally different than mare basalts.

Discussion: Under certain conditions, differentiated impact melt could conceivably produce the distinct stratigraphy observed across SPACA (high-Ca pyroxene lithology overlying Mg-rich pyroxene lithology). However, impact melt cannot account for the regional paucity

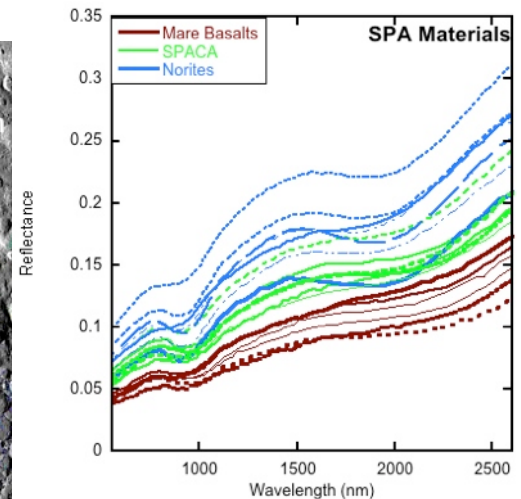


Fig. 3: Example spectra for several SPA materials. The population of flooded, buried, and otherwise modified craters throughout central SPA[15] provide clear evidence of a complex sequence of events including volcanic resurfacing. Finally, the SPACA extends beyond the central depression into the northern smooth terrain: i.e., outside of the primary melt pool. Therefore, it is unlikely that this material represents differentiated impact melt.

Instead, the physical properties of central SPA indicate resurfacing after melt sheet solidification. Volcanic flooding may have been triggered in part by the SPA impact itself, distinct from later mare volcanism. Such a scenario is more consistent with the compositional structure, smooth terrain, and paucity of impact craters throughout SPACA.

Acknowledgements: This analysis is supported through NASA LASER (NNX12AI96G) and SSERVI (NNA14AB01A).

References: [1]Stuart-Alexander, D. E. 1978, *USGS*. [2]Spudis, P. D. et al. 1994, *Sci.*, 266:1848-1851. [3]Garrick-Bethell, I. and M. T. Zuber 2009, *Icar.*, 204:399-408. [4]Melosh, H. J. 1989, *Imp. Crat.*, Oxford Press. [5]Potter, R. W. K. et al. 2012, *Icar.* 220:730-743. [6]Jolliff, B. L. et al. 2000, *J. Geo. Res.* 105:4197-4216. [7]Pieters, C. M. et al. 2001, *J. Geo. Res.* 106:28001-28022. [8]Moriarty, D. M. and C. M. Pieters 2016, *LPSC 47*. [9]Ohtake, M. et al. 2014, *Geo. Res. Let.* 41:2738-2745. [10]Pieters, C. M. et al. 2009, *Curr. Sci.* 96:4:500-505. [11]Smith, D. E. et al. 2010, *Geo. Res. Let.*, 37:L18204. [12]Robinson, M. S. et al. 2010, *Spa. Sci. Rev.*, 150:1-4:81-124. [13]Head, J. W. et al. 2010, *Sci.* 329:1504-1507. [14]Kadish, S. J. et al. 2011, *LPSC XLII*, #1006. [15]Moriarty, D. M. and C. M. Pieters 2015, *Geo. Res. Let.* 42. [16]Moriarty, D. M. and C. M. Pieters (2016), *Met. and Plan. Sci.*, in press. [17]Klima, R. L. et al. 2007, *Met. and Plan. Sci.* 42:2:228-251. [18]Klima, R. L. et al. 2011, *Met. and Plan. Sci.*, 46:3:379-395. [19]Cintala, M. J. and R. A. F. Grieve 1998, *Met. and Plan. Sci.* 33:889-912. [20]Elkins-Tanton, L. T. et al. 2011, *Earth Planet. Sci. Lett.* 304:326-336. [21]Hurwitz, D. M. and D. A. Kring 2014 *J. Geo. Res.* 119:1110-1133. [22]Vaughan, W. M. et al. 2013, *Icar.* 223:749-765. [23]Vaughan, W. M. and J. W. Head 2014, *Plan. Spa. Sci.* 91:101-106. [24]Petro, N. E. et al. 2011, *Geol. Soc. Am.* 477:129-140. [25]Whitten, J. L. and J. W. Head 2014, *Icar.* 247:150-171. [26]Elkins-Tanton, L. T. and B. H. Hager 2005, *Earth Plan. Sci. Let.* 239:219-232. [27]Turner, S. and C. Hawkesworth 1995, *Chem. Geol.* 120:295-314. [28]Morbidelli, A. et al. 2012, *Ear. Plan. Sci. Let.* 355-356:144-151.